

# Enhanced sonocatalytic treatment of ibuprofen by mechanical mixing and reusable magnetic core titanium dioxide



Kyounglim Kang<sup>a</sup>, Min Jang<sup>b,c,\*</sup>, Mingcan Cui<sup>a</sup>, Pengpeng Qiu<sup>a</sup>, Seungmin Na<sup>d</sup>, Younggu Son<sup>e</sup>, Jeehyeong Khim<sup>a,\*</sup>

<sup>a</sup> School of Civil, Environmental and Architectural Engineering, Korea University, Seoul 136-701, Republic of Korea

<sup>b</sup> Department of Civil Engineering, Faculty of Engineering, University of Malaya, Kuala Lumpur 50603, Malaysia

<sup>c</sup> Nanotechnology and Catalysis Research Centre (NANOCAT), University of Malaya, Kuala Lumpur 50603, Malaysia

<sup>d</sup> National Institute of Environmental Research ministry of Environment Nakdong River Environment Research Center, 239-3, Pyeongri, Dasanmyeon,

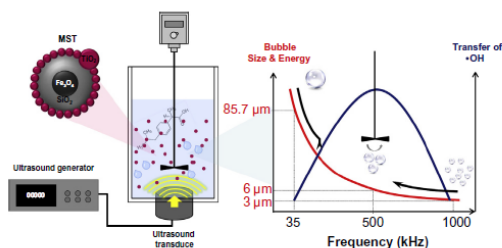
Gonyeongu Gyeongsangbudo 717-873, Republic of Korea

<sup>e</sup> Department of Civil Environmental and Environmental Engineering, Kumoh National Institute of Technology, Daehak-ro 61, Gumi, Gyeongbuk 730-701, Republic of Korea

## HIGHLIGHTS

- MST was synthesized and evaluated as a recyclable sonocatalyst for IBP removal.
- MST coupled sonocatalysis for IBP removal was studied with various parameters.
- Mechanical mixing makes to reverse the US frequency effect on IBP removal.
- MST was almost as effective as commercial TiO<sub>2</sub> and showed a high reusability.

## GRAPHICAL ABSTRACT



## ARTICLE INFO

### Article history:

Received 12 August 2014

Received in revised form 6 October 2014

Accepted 30 October 2014

Available online 21 November 2014

### Keywords:

Magnetically separable titanium dioxide

Ibuprofen

Sonolysis

Sonocatalysis

Mixing

## ABSTRACT

As a reusable sonocatalyst, magnetically separable titanium dioxide (MST) was synthesized by a sol-gel method and was evaluated in the removal of ibuprofen (IBP). MST was carefully characterized by X-ray diffraction (XRD), Fourier transform infrared spectroscopy (FT-IR), N<sub>2</sub> gas isotherms, band-gap energy, magnetization, zeta potential, and particle size distribution. The kinetics of IBP removal by sonolysis or MST-assisted sonocatalysis was systematically evaluated with various operational parameters such as pH, temperature, ultrasound (US) frequency, and mechanical mixing intensity. For the first time, authors found that mechanical mixing had an opposite effect on the oxidation rate constants of IBP removal by sonolysis or sonocatalysis according to US frequency. Specifically, the magnitude orders of oxidation rate constants in sonolysis and sonocatalysis with mixing (350 rpm) were the same (35 > 1000 > 300 > 500 > 700 kHz), but sonolysis without mixing showed the following order: 500 > 1000 > 35 kHz. In addition, the removal rate constant of IBP by sonocatalysis at the lowest US frequency (35 kHz) increased exponentially as the mechanical mixing speed increased. MSM exhibited a high reusability because it has similar rate constants with an average value of  $17 \pm 0.3 \times 10^{-3} \text{ min}^{-1}$  five repetitive kinetic tests.

© 2014 Elsevier B.V. All rights reserved.

## 1. Introduction

Ibuprofen (IBP) is ubiquitous in the environment and has been detected in many water sources and in wastewater [1,2]. An assessment by the World Health Organization (WHO) indicated

\* Corresponding authors at: Department of Civil Engineering, Faculty of Engineering, University of Malaya, Kuala Lumpur 50603, Malaysia (M. Jang). Tel.: +82 2 3290 3318; fax: +82 2 928 7656 (J. Khim).

E-mail addresses: minjang@um.edu.my (M. Jang), hyeong@korea.ac.kr (J. Khim).

that IBP is the leading endocrine disrupting compound (EDC). For example, the detected concentrations of IBP have been higher than those of erythromycin, bleomycin and others. IBP exposure is associated with various health and ecotoxicological risks to the human and aquatic wild life; even very low concentrations have resulted in harmful effects on the human endocrine system and aquatic wild life reproduction [1–4]. Thus, the removal of IBP from water represents an emerging environmental concern.

Recently, energy-based heterogeneous catalysis has received significant attention in the treatment of various organic pollutants. Specifically, because of their high catalytic performance, heterogeneous catalysts have been studied in the removal of EDCs by environmentally friendly wave-energy oxidations such as ultrasound (US) or ultraviolet (UV) irradiation [5,6]. As a representative photocatalyst,  $\text{TiO}_2$  is highly stable, resistant to acidic or alkaline conditions, nontoxic, safe, inexpensive, and has a strong redox reaction. Thus,  $\text{TiO}_2$  is known as the best material for oxidizing organic pollutants [7,8]. When  $\text{TiO}_2$  is applied in UV-based oxidation, various organic pollutants can be degraded or even mineralized into  $\text{CO}_2$  and  $\text{H}_2\text{O}$  because of the production of hydroxyl radicals ( $\cdot\text{OH}$ ), which have a strong oxidation potential (2.8 V) [9]. However, the use of  $\text{TiO}_2$ /UV is difficult with nontransparent and highly turbid wastewater [10]. On the other hand, US can decompose organic pollutants by cavitation and photocatalysis and can penetrate turbid aqueous media. The penetration depth of UV is a few millimeters, while that of US is 15–20 cm [11]. Furthermore,  $\cdot\text{OH}$  generation increases when  $\text{TiO}_2$  is combined with US. For example,  $\text{TiO}_2$ -assisted US exhibited a 2–4 times higher decomposition efficiency of methyl orange than US alone [12,13]. The pore volume of  $\text{TiO}_2$  supplies additional nuclei to increase the number of cavitation bubbles, eventually increasing the  $\cdot\text{OH}$  generation when the bubbles burst [14]. In addition to the cavitation effect, UV emission by the sonoluminescence of US excites  $\text{TiO}_2$  to produce additional  $\cdot\text{OH}$  through the decomposition of water molecules by holes ( $h^\cdot$ ) [15].

Until now, various  $\text{TiO}_2$ -based sonocatalysts have been synthesized and applied in conjunction with US, and various operational parameters have been studied [16–19]. Although these studies focused on different sonocatalysts based on  $\text{TiO}_2$ , there is no study on reusable sonocatalysts or how to enhance the oxidation efficiency of sonolysis or sonocatalysis by mechanical mixing. In fact, the recovery and reusability of sonocatalysts are the key issues in resolving the applicability for the industrial-scale treatment processes [20]. Several techniques are available for the recovery and reuse of catalysts, including coagulation by using aluminum chloride [21], separation using ultrafiltration (UF) membranes [8], film-type catalysts [22], and magnetic catalysts. Among these techniques, the most effective and simplest method involves the recovery and reuse of magnetically active catalysts. Although some studies on magnetic  $\text{TiO}_2$  prepared by coating  $\text{TiO}_2$  on the magnetic core of  $\text{Fe}_3\text{O}_4$  or  $\text{Fe}_2\text{O}_3$  were reported, they were limited to UV oxidation processes [20,23–28].

The objectives of this study were to synthesize magnetically separable titanium dioxide (MST), and apply it in a US oxidation system for the removal of IBP in aqueous media. Several batch tests were conducted to investigate the effect of important operational parameters such as US frequency, mechanical stirring, pH and temperature, as well as the degree of recovery and reusability of MST.

## 2. Materials and methods

### 2.1. Materials

Magnetite nanopowder ( $\text{Fe}_3\text{O}_4$ , ~50 nm, Aldrich), tetraethyl orthosilicate (TEOS, grade 99%, Aldrich), titanium butoxide purum (TBT, grade  $\geq 97\%$ , Fluka), aqueous ammonia solution (30%,

Duksan, Korea), and ethanol (grade 99.9%, Duksan, Korea) were obtained and utilized to synthesize MST. Ibuprofen (IBP, grade 98%) was purchased from Aldrich (USA). In order to compare the performance of synthesized MST, nanosized  $\text{TiO}_2$  (Degussa, P25, anatase/rutile = 75/25%) was obtained and used for IBP oxidation.

### 2.2. Sonocatalysis experiment

#### 2.2.1. MST preparation and sonocatalysis reactor setup

As a sonocatalyst, MST was prepared and used for sonocatalysis reactor. The preparation method of  $\text{SiO}_2$  coated nano-magnetite and MST were described in Supporting information (SI). The setup of the sonocatalytic reactor is shown in Fig. 1. A glass, horn-type sonoreactor ( $\Phi 100 \times H 115$  mm, total volume: 0.8 L, effective volume: 0.5 L) made of Pyrex with a single piezoelectric transducer module (PZT, Tamura, Japan) was used for the kinetic evaluation of the sonocatalytic removal of IBP. The transducer was coupled with an ultrasonic generator (Mirae Ultrasonic MEGA-100, Korea). A stirrer (MS 3060D) was used for the mechanical mixing. The temperature in the solution was maintained with a temperature controller (RC-10V, Immersion circulator).

#### 2.2.2. Sonolysis and sonocatalysis for IBP oxidation

The IBP stock solution ( $1000 \text{ mg L}^{-1}$ ) was made by dissolving 0.1 g of IBP powder in 100 mL of methanol. Then, IBP containing water ( $1 \text{ mg L}^{-1}$ ) was prepared by adding 5 mL of IBP stock solution into 5 L of deionized water. After adding 1.5 g of MST into 500 mL of the IBP solution ( $1 \text{ mg L}^{-1}$ ) [29], the suspension was homogeneously mixed using a stirrer at a constant speed, temperature ( $24 \pm 1^\circ\text{C}$ ), and calorimetric power density ( $41 \text{ W L}^{-1}$ ).

Batch tests were conducted based on the aforementioned conditions to investigate the effect of the US frequency at 35, 300, 500, 700, and 1000 kHz on the oxidative removal of IBP and  $\text{I}_3^-$  production. For these tests, the pH and mechanical mixing speeds were fixed at  $6.6 \pm 0.5$  and 350 rpm, respectively. At either 35 or 500 kHz, the effect of mechanical stirring (0, 150, 250, 350 rpm) on the removal of IBP was also determined at  $\text{pH } 6.6 \pm 0.5$ . To determine the effect of pH, batch tests were conducted by adjusting the initial pH of the suspension to 3, 4, 4.9, 5.5, or 6.6 using  $1 \text{ mol L}^{-1}$  of HCl at a fixed frequency of 35 kHz. The effect of temperature on the IBP removal was also investigated at 25, 40, or  $55 \pm 1^\circ\text{C}$  using a temperature controller with a water jacket. For these tests, the US frequency, pH, and mechanical mixing speed were fixed at 35 kHz,  $6.6 \pm 0.5$ , and 350 rpm, respectively. Under the same conditions described above, P25 was applied to the sonocatalytic degradation of IBP and its performance was compared to that of MST.

#### 2.2.3. Reusability tests of MST

Following the sonocatalytic oxidation reaction, MST was collected by centrifuging the suspension. Then, the separated MST was washed at least three times with distilled water and subsequently dried at room temperature. The dried MST was reused for the subsequent sonocatalytic oxidation process conducted under the same conditions: 500 mL of IBP solution ( $1 \text{ mg L}^{-1}$ ) and reclaimed MST ( $3 \text{ g L}^{-1}$ ). With five cycles of MST reusability, the sonocatalytic oxidation efficiencies of IBP were investigated in triplicate tests for 1 h.

### 2.3. Analysis

#### 2.3.1. Characterization

To ascertain the physicochemical properties of MST, several analyses such as BET surface area, XRD, FT-IR, band-gap energy, magnetization, particle distribution were conducted. All information of analytical methods was in SI.

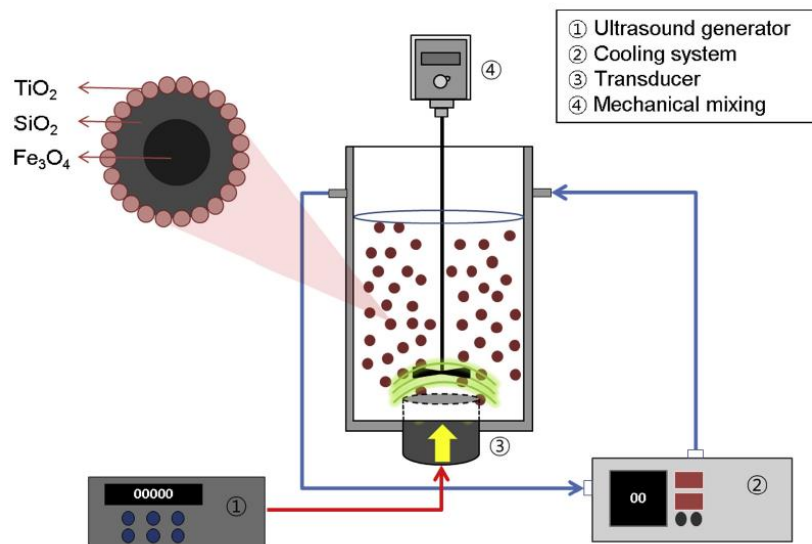


Fig. 1. Schematic diagram of a sonocatalytic reactor.

### 2.3.2. Analytical methodologies

Samples (2 mL) were withdrawn from the sonocatalytic reactor every 10 min for 1 h, and then filtered using a 0.45- $\mu\text{m}$  pore filter. The IBP content of the filtrate was analyzed by liquid chromatography (LC, Agilent 1260) coupled with an ECLIPSEXRB-C18 (250  $\times$  4.6 mm, 5- $\mu\text{m}$  beads) column and a diode array detector (G4212B 1260 DAD,  $\lambda = 222 \text{ nm}$ ). The mobile phase was composed of acetonitrile (purity, 99.9%) and orthophosphoric acid (0.2 M) in a ratio of 35:65, and its flow rate was set to 1 mL  $\text{min}^{-1}$ .

### 2.3.3. Kinetic analysis and thermodynamic calculation

The kinetic constants for each test, thermodynamic parameters (i.e., enthalpy, entropy, and activation energy), and photonic efficiencies were determined using the analyzed concentrations of IBP. All explanation for pseudo-first-order kinetic model, thermodynamic parameters and US power density was denoted in SI.

## 3. Results and discussion

### 3.1. Characterization of MST

#### 3.1.1. XRD and FT-IR analyses

Fig. S1 shows the XRD analysis of  $\text{Fe}_3\text{O}_4$ ,  $\text{Fe}_3\text{O}_4\text{-SiO}_2$ , MST, and analogous  $\text{TiO}_2$  (P25) for comparison.  $\text{Fe}_3\text{O}_4$  peaks appeared at 30.21°, 35.55°, 43.12°, 53.40°, 57.19°, and 62.60°, corresponding to the (220), (311), (400), (422), (511), and (440) reflection phases. These peaks were indexed as the magnetite phase (JCPDS 19-0629). Meanwhile,  $\text{TiO}_2$  (P25) peaks were indexed to the anatase (JCPDS 21-1272) and rutile phases (JCPDS 21-1276), respectively. Specifically, the peaks of the anatase phase appeared at 25.43°, 37.92°, 48.03°, 53.97°, 55.05°, and 68.80°, corresponding to the (101), (112), (200), (105), (211), and (116) reflections, respectively. The rutile phase of  $\text{TiO}_2$  was also detected at 27.45°, 36.08°, 41.27°, and 62.70°, which were indexed to the (110), (101), (111), and (204) reflections, respectively.  $\text{Fe}_3\text{O}_4\text{-SiO}_2$  exhibited peaks at 23.2°, 26.6°, 30.21°, 35.55°, 43.12°, 53.40°, 57.19° and 62.60°, which were attributed to the (101), (011),

(220), (311), (400), (422), (511), and (440) reflections of  $\text{Fe}_3\text{O}_4$  (220, 311, 400, 422, 511, 440) and  $\text{SiO}_2$  (101 and 011), respectively. The MSTs displayed peaks at 25.43°, 27.45°, 30.21°, 35.55°, 37.92°, 48.03°, 53.97°, 55.05°, 62.70°, and 68.80°, attributed to the (101), (110), (220), (311), (112), (200), (105), (211), (204), and (116) reflections. Among those, the (220 and 311) and (101, 110, 112, 200, 105, 211, 204, and 116) reflections suggested the phases of  $\text{Fe}_3\text{O}_4$  and  $\text{TiO}_2$ , respectively. As a result of phase identification for  $\text{TiO}_2$ , the anatase and rutile compositional ratios in MST were 90% and 10% by weight, respectively.

FT-IR was used to characterize the composition and structure of MST (Fig. S2). The signal at  $\sim 800$  and  $1080 \text{ cm}^{-1}$  corresponded to the symmetric vibration of Si-O-Si and asymmetric stretching vibration of the Si-O-Si bond, while those at 940-960 and  $650 \text{ cm}^{-1}$  were assigned to the Si-O-Ti vibration and originated from the Ti-O-Ti bond [30,31]. Thus, based on the results of FT-IR and XRD, silica was presented as an amorphous phase. The bands at  $\sim 1630$  and  $3370 \text{ cm}^{-1}$  were attributed to the bending vibration of the hydroxyl groups.

#### 3.1.2. BET and band-gap energy analysis

Pore properties such as surface area, pore volume, and size have a close relationship with the micro-bubble nuclei supplement and increase the numbers of cavitation bubbles and production of  $\cdot\text{OH}$ , sequentially enhancing the oxidation rate.  $\text{N}_2$  gas isotherm analysis revealed that the BET surface area, pore diameter and volume of the MST were  $7.8 \text{ m}^2 \text{ g}^{-1}$ , 12.5 nm, and  $0.02 \text{ cm}^3 \text{ g}^{-1}$ , respectively (Table S1). Fig. S3 shows adsorption-desorption isotherms and pore size distribution of MST, indicating that heterogeneous inter-particle pores are major structures. P25 had a BET surface area ( $63 \text{ m}^2 \text{ g}^{-1}$ ), which was 8.1 times greater than that of MST, while it had a three times larger pore volume ( $0.06 \text{ cm}^3 \text{ g}^{-1}$ ). The differences in the surface area and pore volume between P25 and MST were reasonable, because the particle size (50 nm) of single sphere P25 is much smaller than that of MST (362 nm), which is not composed of  $\text{TiO}_2$  only (Fig. S4). Using a UV/Vis spectrometer, the band-gap energies of MST (3.1 V) and P25 (3.2 V) were analyzed.



Accordingly, the band-gap energy of MST was lower than that of P25 (Fig. S5).

### 3.1.3. Magnetization of MSTs

Magnetization profiles of  $\text{Fe}_3\text{O}_4$ ,  $\text{Fe}_3\text{O}_4\text{-SiO}_2$ , and the MSTs were acquired at room temperature (300 K) (Fig. S6). The saturation magnetization value of  $\text{Fe}_3\text{O}_4$  was  $72.0 \text{ emu g}^{-1}$ , which was in good agreement with other references [32,33]. Although smaller catalysts may exhibit higher sonocatalytic activities because of increased surface areas, a small size may be detrimental in magnetic separation. Given that the magnetic force in a field gradient acts proportionally to particle size, fine magnetic particles cannot be separated when the magnetic force is insufficient to overcome their Brownian motion [34].  $\text{Fe}_3\text{O}_4\text{-SiO}_2$  exhibited a magnetization value of  $11.2 \text{ emu g}^{-1}$  while that of MST was less ( $2.5 \text{ emu g}^{-1}$ ). Compared to the core material ( $\text{Fe}_3\text{O}_4$ ), the magnetization values of  $\text{Fe}_3\text{O}_4\text{-SiO}_2$  and MST were smaller because of the volume contribution of the nonmagnetic coating layer ( $\text{TiO}_2$  and  $\text{SiO}_2$ ) to the total volume of the individual particles.

### 3.2. Effect of US frequency and mechanical mixing

It is important to find out the effects of the US frequency on the oxidative removal of organic contaminants, because physical effects such as microjets, microtrimming, and shock waves and the production rate of  $\cdot\text{OH}$  could vary according to the US frequency. As the frequency decreases, the size of the cavitation bubbles increase, but the transfer of  $\cdot\text{OH}$  produced during the burst of cavitation into external organic matter reduces due to the decreases of temperature and pressure. When the frequency increases to the critical condition that maximizes the temperature and pressure of bubbles, the mass transfer of  $\cdot\text{OH}$  also can be the highest because of the optimum size of cavitation. On the contrary, however, the temperature and pressure can decrease at above the critical point of frequency as bubbles become smaller [35–37]. Therefore, ultrasonic oxidation of organic matters can be significantly enhanced at the optimum frequency condition [35]. When a sonocatalyst is applied in US, the effect of the frequency could be more complicated because the extent of homogeneous dispersion of the catalyst could be varied by microjets, microtrimming, and shock waves. Accordingly, because mechanical mixing should be applied to homogeneously distribute the sonocatalyst in the reactor, it is essential to determine the optimal frequency that could differ from that in sonolysis.

To establish the effect of the US frequency in this study, the sonolytic or sonocatalytic oxidation of IBP was conducted with frequencies ranging from 35 to 1000 kHz and under fixed operational conditions (Section 2.2.2). The optimum frequency was determined by determining the constants of IBP removal rate and  $\text{I}_3^-$  production rate using pseudo-first-order kinetic model.

For sonocatalysis (Fig. 2A and B) with mechanical stirring (350 rpm), the removal rate constants of IBP at 35, 300, 500, 700, and 1000 kHz (US frequency) were  $17.3 \times 10^{-3}$ ,  $7.2 \times 10^{-3}$ ,  $6.2 \times 10^{-3}$ ,  $4.5 \times 10^{-3}$ , and  $14.8 \times 10^{-3} \text{ min}^{-1}$  and the  $\text{I}_3^-$  production rate constants were 1.009, 0.21, 0.205, 0.160, and  $0.800 \text{ mM min}^{-1}$ , respectively. When MST was not applied, the rate constants of IBP removal were  $15.3 \times 10^{-3}$ ,  $3.2 \times 10^{-3}$ ,  $3.7 \times 10^{-3}$ ,  $3.0 \times 10^{-3}$ , and  $13.9 \times 10^{-3} \text{ min}^{-1}$  and the rate constants of  $\text{I}_3^-$  production were 0.54, 0.17, 0.172, 0.116, and  $0.437 \text{ mM min}^{-1}$ , respectively (Fig. 2C and D). Thus, the sonolysis of IBP was slower than that in sonocatalysis. However, the magnitude of both parameters in sonolysis and sonocatalysis were the same ( $35 > 1000 > 300 > 500 > 700 \text{ kHz}$ ) so that the highest rates of IBP oxidation and  $\text{I}_3^-$  production were obtained at 35 kHz. Accordingly, it can conclude that  $\cdot\text{OH}$  production is a dominant action for IBP removal.

For sonolysis without mixing, the IBP removal rate constant at 500 kHz ( $12.7 \times 10^{-3} \text{ min}^{-1}$ ) was higher than those at 35 kHz ( $4.1 \times 10^{-3} \text{ min}^{-1}$ ) and 1000 kHz ( $8.1 \times 10^{-3} \text{ min}^{-1}$ ), indicating that 500 kHz was the optimum frequency. This result coincided with that of Kang et al. [35], in which methyl tert-butyl ether (MEBE) was oxidized by sonolysis and the optimized US frequency was found to be 300–500 kHz (Fig. 2E). Kanthale, Ashokkumar and Grieser [38] also reported that the optimal frequency could arise because of the changes in the bubble sizes, ratio of maximum radius to initial radius of the bubble at the collapse,  $T_{\text{max}}$ , and sonoluminescence (SL) intensity.

Notably, when mechanical mixing was applied, the effect of the US frequency on the kinetic constants of IBP removal by sonolysis was the opposite. Accordingly, mechanical stirring had a significant effect on the removal of IBP by sonolysis or sonocatalysis.

To determine the effect of mechanical stirring (0, 150, 250, 350 rpm), batch tests of IBP removal by sonolysis or sonocatalysis using MST were performed at US frequencies of either 35 or 500 kHz and a fixed pH ( $6.6 \pm 0.5$ ). The operational conditions are described in Section 2.2.2.

With a US frequency of 35 kHz, the rate constants of IBP removal by sonocatalysis with 0, 150, 250, and 350 rpm of mechanical mixing were  $6.6 \times 10^{-3}$ ,  $8.3 \times 10^{-3}$ ,  $11.5 \times 10^{-3}$ , and  $17.3 \times 10^{-3} \text{ min}^{-1}$ , respectively (Fig. 3A). Therefore, the removal rate of IBP exponentially increased as the mixing speed increased. At 500 kHz, the rate constants with 0, 150, 250, and 350 rpm mixing speed were  $4 \times 10^{-3}$ ,  $5.4 \times 10^{-3}$ ,  $6.9 \times 10^{-3}$ , and  $6.2 \times 10^{-3} \text{ min}^{-1}$ . As such, they did not significantly increase with increased mixing speeds (Fig. 3B).

In sonolysis at 35 kHz, the rate constants of IBP removal were  $4.1 \times 10^{-3}$ ,  $7.8 \times 10^{-3}$ ,  $10.3 \times 10^{-3}$ , and  $15.3 \times 10^{-3} \text{ min}^{-1}$  at 0, 150, 250, and 350 rpm of mechanical mixing, respectively (Fig. 3C). In sonocatalysis at 35 kHz, the removal rate of IBP increased as the mixing speed increased. However, at 500 kHz, the rate constants of IBP removal by sonolysis with 0, 150, 250, and 350 rpm of mechanical mixing were  $12.7 \times 10^{-3}$ ,  $6.8 \times 10^{-3}$ ,  $4.4 \times 10^{-3}$ , and  $3.7 \times 10^{-3} \text{ min}^{-1}$ , respectively. Therefore, the removal of IBP decreased with increased mixing speeds (Fig. 3D). Fig. 3(E) shows the overall results of IBP removal kinetic constants by sonolysis and sonocatalysis at various mixing speeds and a constant frequency of either 35 or 500 kHz.

As shown in Figs. 2 and 3, the US frequency and mechanical mixing can have noteworthy effects on the speed of IBP removal by sonolysis or sonocatalysis. Apparently, these operational parameters are closely related to the diameter of the cavitation bubbles. Based on Minnaert's equation (resonance bubble size,  $R_{\text{res}} = 3/F$ ), the diameter of cavitation bubbles decreases as the frequency increases [39]. Theoretically, the diameter (85.7  $\mu\text{m}$ ) of the bubbles at 35 kHz is about 14.3 times larger than that (6  $\mu\text{m}$ ) at 500 kHz [39]. Therefore, without stirring, 500 kHz led to a faster removal of IBP than 35 kHz, as shown at Figs. 2(E) and 3(E). The rate constant of IBP removal by sonolysis at 500 kHz ( $12.7 \times 10^{-3} \text{ min}^{-1}$ ) was about 3.1 times higher than that at 35 kHz ( $4.1 \times 10^{-3} \text{ min}^{-1}$ ). Nevertheless, when mechanical mixing was applied, the kinetic results were reversed. Hypothetically, larger bubbles (85.7  $\mu\text{m}$ ) created at a low frequency (i.e., 35 kHz) by US can split into smaller bubbles by mechanical mixing. Accordingly, the number of bubbles and  $\cdot\text{OH}$  production increases. On the other hand, fine bubbles (6  $\mu\text{m}$ ) produced at 500 kHz have can potentially combine into larger bubbles with mechanical stirring, rather than splitting to smaller bubbles. Moreover, this causes a decrease in the number of bubbles and  $\cdot\text{OH}$  production, which consequentially decelerates the reaction rate [40]. With a US frequency of 1000 kHz, the size of the bubbles is small (about 3  $\mu\text{m}$ ); mechanical mixing might increase their size to an appropriate scale to enhance the oxidation speed.

Link to Full-Text Articles:

<http://www.sciencedirect.com/science/article/pii/S1385894714014387>